JOURNAL OF APPLIED ELECTROCHEMISTRY 22 (1992) 1155–1160

Experimental investigation of the primary and secondary current distribution in a rotating cylinder Hull cell

C. MADORE, M. MATLOSZ, D. LANDOLT

Laboratoire de Métallurgie Chimique, Département des Matériaux, Ecole Polytechnique Fédérale de Lausanne, MX-C Ecublens, CH-1015 Lausanne, Switzerland

Received 21 February 1992

A rotating cylinder cell having a nonuniform current distribution similar to the traditional Hull cell is presented. The rotating cylinder Hull (RCH) cell consists of an inner cylinder electrode coaxial with a stationary outer insulating tube. Due to its well-defined, uniform mass-transfer distribution, whose magnitude can be easily varied, this cell can be used to study processes involving current distribution and mass-transfer effects simultaneously. Primary and secondary current distributions along the rotating electrode have been calculated and experimentally verified by depositing copper.

List of symbols

- c distance between the cathode and the insulating tube (cm)
- F Faraday's constant (96 484.6 C mol^{-1})
- h cathode length (cm)
- i local current density (A cm^{-2})
- i_L limiting current density (A cm^{-2})
- i_{ave} average current density along the cathode (A cm^{-2})
- i_0 exchange current density (A cm^{-2})
- I total current (A)
- M atomic weight of copper (63.54 g mol^{-1})
- n valence
- r_p polarization resistance (Ω)
- t deposition time (s)
- V_c cathode potential (V)
- Wa_T Wagner number for a Tafel kinetic approximation
- x/h dimensionless distance along the cathode surface
- z atomic number

Greek symbols

- β_a anodic Tafel constant (V)
- β_c cathodic Tafel constant (V)
- Φ solution potential (V)
- η overpotential at the cathode surface (V)
- ρ density of copper (8.86 g cm^{-3})
- κ electrolyte conductivity (Ω cm^{-1})
- μ deposit thickness (cm)
- μ_{ave} average deposit thickness (cm)
- ξ surface normal (cm)

1. Introduction

The traditional Hull cell [1] is a trapezoidal structure in which the cathode is situated at an oblique angle with respect to the anode. The cell allows exploration of the variation in the appearance of an electrodeposit over a wide range of current densities along the cathode surface in order to determine optimal electroplating conditions [2]. Although it is useful in many applications, a shortcoming of the Hull cell is the absence of controlled mass-transport conditions. Consequently the cell cannot be used to study procesees that involve a mass-transfer limited step. In order to overcome this handicap, some authors have proposed different Hull-type cells that include controlled hydrodynamic conditions. Graham and Pinkerton [3] built a rotating cylinder placed coaxially with a stationary conical anode. The current distribution along the cathode examined in their studies, however, was significantly more uniform than that obtained in the traditional Hull cell. Kadija *et al.* [4] developed a hydrodynamically controlled Hull cell using a rotating cylinder with the anode placed above the cathode on the cylinder. They obtained a current distribution similar to that of the Hull cell by using insulator baffles. Lu [5] proposed several designs using conical and cylindrical electrodes. The described cell configurations, however, were either empirical or of complex geometry and therefore had limited applicability.

A simple design for a cell with well characterized mass-transport properties and a primary current distribution similiar to that of the Hull cell has been proposed in a recent paper [6]. The proposed rotating cylinder Hull (RCH) cell consists of an inner rotating cylinder electrode and a stationary, concentric outer insulating tube. The counterelectrode is placed at one end of the cell to provide a nonuniform current distribution along the rotating cathode. In order to avoid an undesirable sharp increase of current at the

0021-891X

working electrode edges, the active part of the rotating cylinder is recessed slightly.

The primary current distribution along the rotating cylinder electrode was calculated for varying geometrical dimensions and was found to be mainly determined by the ratio h/c, where h is the length of the working electrode and c the distance between the inner cylinder and the insulating cylindrical tube. A value of $h/c = 3$ was found to give a primary current distribution that varies, similarly to that in the Hull cell, by about one order of magnitude from one end of the cathode to the other. Moreover, the study showed that the distance between the counterelectrode and the leading edge of the cathode had no significant influence on the current distribution.

The use of an RCH for studies involving the effects of current density variations on electrochemical reactions presents many advantages. A rotating cylinder electrode has a uniform high mass-transport rate [7, 8] and the correlation between the limiting current density and the rotation speed is well established [9]. The RCH cell can thus be used for evaluating high speed plating processes [10]. In addition, a rotating cylinder can be easily segmented, facilitating the analysis of the deposits. Unlike planar electrodes in channel flow, edge effects, either in the hydrodynamics or current distribution, are minimal, and the cell is easy to build.

The aim of this work was to build a cell according to the geometry described above and to verify experimentally the current distribution along the cathode, including the effects of kinetics. Experimental results for copper deposition from an acid sulphate bath have been compared with numerical simulations.

2. Current distribution calculation

In the absence of concentration gradients in the electrolyte, the current density, i, at any point in the cell is related to the gradient of the electric potential through Ohm's law:

$$i = -\kappa \nabla \Phi \tag{1}$$

where κ is the electrolyte conductivity and Φ the local potential in the electrolyte. The potential distribution is obtained from the solution of Laplace's equation,

$$\nabla^2 \Phi = 0 \tag{2}$$

subject to the following boundary conditions along the anode, the cathode and the insulating walls:

$$\Phi = V_a \tag{3}$$

$$\Phi = V_c \tag{4}$$

$$\frac{\partial \Phi}{\partial \xi} = 0 \tag{5}$$

where V_a and V_c are anode and cathode potentials and where ξ is the normal to the cathode surface. The local current density at the cathode surface is evaluated from the local potential gradient perpendicular to the surface.

The calculation of the secondary current distribution takes the reaction kinetics into consideration through the cathode boundary condition:

$$-\kappa \frac{\partial \Phi}{\partial \xi} = i(\Phi, V_c) \tag{6}$$

The local current density at the electrode surface is a function of Φ and V_c. When a single species is electrodeposited, the kinetics at the electrode surface can be represented by the Butler–Volmer equation

$$i = i_0\{\exp(\eta/\beta_a) - \exp(-\eta/\beta_c)\} \tag{7}$$

$$\eta = V_c - \Phi \tag{8}$$

where the potential Φ is the reversible, open circuit potential for copper ($\Phi = -380\,\text{mV}$ against a $Hg/HgSO_4$ reference) i_0, an exchange current density, η the overpotential, and β_a and β_c anodic and cathodic Tafel constants. If the cathode potential is high, only the cathodic term in Equation 7 is important (Tafel approximation):

$$i = -i_0 \exp(-\eta/\beta_c) \tag{9}$$

For the Tafel approximation, it can be shown that the secondary current distribution is a function of the numerical value of a single dimensionless parameter, the Wagner number [11], defined as:

$$Wa_T = \frac{\beta_c \kappa}{|i_{ave}| h} \tag{10}$$

where $|i_{ave}|$ is the absolute value of the average current density. As the Wagner number increases, the current distribution becomes more uniform. The primary current distribution corresponds to $Wa_T \to 0$, and is attained when $|i_{ave}|$ and h are high. In order to study the primary current distribution ($Wa_T \to 0$), large cell dimensions and/or high current densities are required. Nevertheless, in order to prevent any effect of mass-transport, the ratio of average deposition current density to the limiting current density i_{ave}/i_L should be as small as possible. The high convection rates obtained at the rotating cylinder electrode allow the primary current distribution to be approached without interference from mass-transfer limitations.

In this work, secondary current distributions have been calculated with a boundary element method (BEM) for an axisymmetric geometry. The principle of this method is described by Brebbia [12] and details of the calculations for the present study are discussed by Matlosz *et al.* [13, 14] including the axisymmetric case. It should be noted that the secondary current distribution calculation involves the nonlinear boundary condition (Equation 6). Hence, an iterative procedure must be added to the primary current distribution calculation.

3. Experimental details

3.1. *The cell*

The total length of the inner rotating cylinder is 15 cm with a working electrode portion 1.5 cm in diameter and 6 cm in length (Fig. 1). The remainder of the

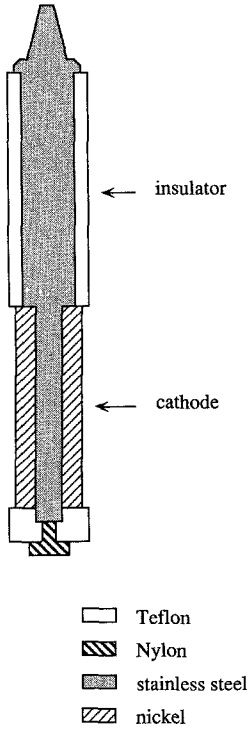

Fig. 1. Rotating cylinder electrode.

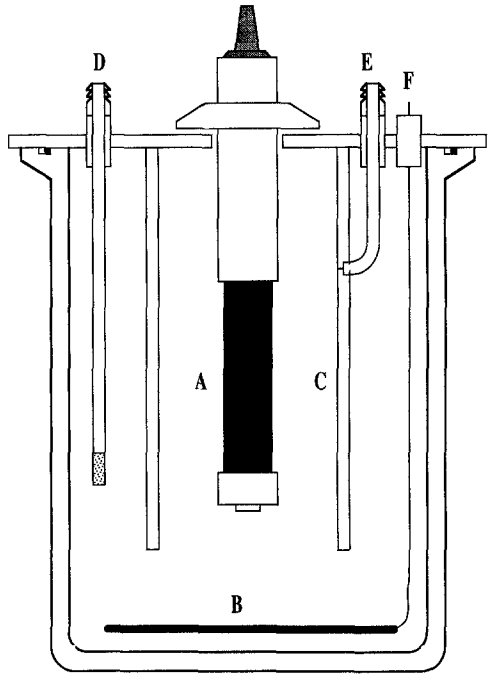

Fig. 2. Illustration of the experimental cell. Cathode (A), anode (B), insulating cylinder wall (plexiglass) (C), gas sparger (D), reference electrode (E), electrical contact (F). Insulating parts of the cylinder are Teflon.

cylinder, the upper 7 cm and the lower 1 cm, is covered with Teflon insulation, and the lower Teflon part is fitted with a nylon screw to permit removal of the electrode. The active electrode area is bounded by Teflon sleeves protruding 0.25 cm from the electrode surface and forming a right angle with it. As discussed earlier, the sleeves are added to eliminate edge effects on the current distribution. The upper end of the cylinder is attached to the motor shaft.

Figure 2 shows the design of the cell. The cylinder is immersed in a Pyrex jacketed reaction vessel of 1 dm^3 volume thermostated by recirculating water to maintain the bath temperature. The active portion of the electrode is submerged about 4 cm below the electrolye surface, and the top of the vessel is covered by a plexiglass cover with an O-ring seal. A Plexiglass tube 5.5 cm in diameter and 12 cm in length, concentric with the rotating cylinder electrode, is attached to the cover. The bottom of the cylindrical insulating wall is open and is situated about 5 cm above the vessel bottom so that the electrolyte can flow between the intercylinder space and the remaining eletrolyte volume. The rotation of the cylinder assures good mixing of the electrolyte. During the experiments, the cell was set on a jack that could be lowered to permit replacement of the rotating cylinder electrode. The lower end of the rotating cylinder electrode was positioned 1 cm above the bottom insulating tube. In this configuration, the current flows through the insulating tube opening, whose radius determines the current distribution. Though the anode can be placed anywhere outside the insulating tube, anode placement around the outside of the tube is preferable to placement below the tube opening when gas evolution occurs at the anode.

For copper deposition, the working electrode was a nickel cylinder (Nickel 201, 99.9%) and the counter-electrode a pure copper disk (Cu 99.99%) 8 cm in diameter placed below the tube opening. When needed, a mercury/mercurous sulphate reference electrode was connected through a small hole in the insulating tube, 1 cm above the working electrode end opposite the counterelectrode. For a reference electrode so positioned, the ohmic drop is minimal.

Electrical current was passed through a mercury contact above the rotator shaft. The current and potential were controlled by an Amel model 555 potentiostat/galvanostat (12 V, 10 A) monitored by an Amel model 566 function generator. The current was measured with a Keithley model 197 multimeter and the potential, when measured, by a Keithley model 617 electrometer. The current was stable to within 0.05% in galvanostatic mode. Data acquisition was performed with an HP 340 microprocessor computer workstation.

3.2. *Copper deposition*

Copper was deposited from an acid sulphate bath of 0.5 M $CuSO_4$ and 1 M H_2SO_4, prepared from reagent grade chemicals (Merck) and doubly-distilled water. A high copper concentration was used to minimize the influence of mass-transport and a high acid concentration to increase the bath conductivity and prevent oxide formation at the anode. Prior to each deposition experiment, the eletrolyte was sparged with nitrogen gas for at least 30 min. To improve the reproducibility of the deposit morphology, freshly prepared electrolyte baths were preelectrolysed before use [15]. All deposits were plated at a constant temperature of 25° C and a cylinder rotation speed of 1250 r.p.m., corresponding

Table 1. Current densities and the corresponding deposition times for copper plating

$\|i_{ave}\|$/mA cm^{-2}	i_{ave}/i_L/%	t/min	Wa_T
2	0.5	212	1.00
10	3	42.3	0.20
35	9	12.1	0.06
75	20	4.2	0.03

to a limiting current density of 378 mA cm^{-2}. Prior to deposition, the nickel cylinder cathode was polished with 600 grit sandpaper and washed with soap. It was then cathodically prepolarized in 0.1 M H_2SO_4 for 1 min at 250 mA cm^{-2} and rinsed with distilled water. The temperature was controlled to within two degrees using a temperature controller.

Deposition was performed galvanostatically at average current densities ranging from 2 mA cm^{-2} to 75 mA cm^{-2} corresponding to Wagner numbers between 1.0 and 0.03 (Table 1). The total charge passed through the cell was 692.6 C, corresponding to an average deposit thickness of 9.3 μm. The highest current density employed corresponded to about 20% of the limiting current density. Consequently, the effect of mass-transport could be safely neglected. This was further confirmed by a series of scanning electron micrographs taken at different positions along the cylinder. In all cases, no dendritic or globular formations were observed even for the highest current densities. Current efficiency for copper deposition as measured by weight gain experiments was found to be approximately 100% for all deposits.

3.3. *Thickness analysis with X-ray fluorescence*

Thickness measurements were performed with a Fischeroscope X-ray 1600/2. The X-ray fluorescence signal permits copper thickness determination in the range of 0.5 to 25 μm. Since copper and nickel have similar atomic numbers (z = 29 and z = 28, respectively) a cobalt filter was used to improve the separation of their two X-ray fluorescence peaks. The accuracy depends on measurement time and deposit thickness. Here, a measurement time of 10 s gave an accuracy of 5% for thicknesses between 2 and 25 μm. Twenty-three equidistant measurement points were taken along four evenly spaced lines, parallel to the cylinder axis (Fig. 3).

3.4. *Copper deposition kinetics*

The kinetic parameters for copper deposition were measured both from polarization curves and impedance measurements. A nickel rotating disk electrode of 0.1 cm^2 surface area, preplated with copper, was used in both cases. In order to neglect the error on the measurement of Tafel parameters due to nonuniform current distribution at a disk electrode the reference electrode was placed at a distance greater than three times the disk electrode diameter [16]. Prior to each experiment, a 5 μm thick copper layer was deposited at a current density of 20 mA cm^{-2}.

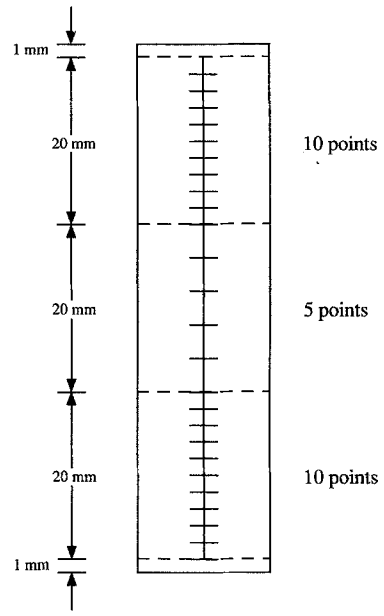

Fig. 3. The twenty-three positions along the cylinder for thickness measurement. The points are evenly spaced in each section.

Polarization curves in the linear and Tafel regions were obtained by sweeping the potential at a rate of 0.5 mV s^{-1} in the linear region and 2 mV s^{-1} in the Tafel region. Polarization resistance and Tafel constants were estimated from the slopes dV_c/dI, where V_c is the applied potential and I the measured total current. Impedance measurements were performed in the frequency range 10^{-3} Hz to 10^4 Hz with a Solartron 1255 frequency response analyzer connected to a Solartron ECI 1286 potentiostat monitored with an HP 9836U microprocessor computer. The values for the polarization resistance and the electrolyte resistance were obtained by extrapolating the Nyquist semi-circle at low and high frequencies respectively. A stable response was obtained by superimposing on the sinusoidal signal a cathodic bias of 40 mV. The anodic and cathodic Tafel constants were found to be β_a = 20 mV and β_c = 45 mV. The exchange current density i_0 and the electrolyte resistance were estimated at 2 mA cm^{-2} and 0.35 Ω cm^2.

4. Results

In Fig. 4, the experimentally measured dimensionless thickness $\mu(x/h)/\mu_{ave}$ and the calculated dimensionless current density $i(x/h)/i_{ave}$ are represented as a function of the dimensionless length x/h along the cathode. The deposit thickness is related to the current density through Faraday's law:

$$\mu(x/h) = \frac{Mt}{nF\rho} i(x/h) \qquad (11)$$

where M is the atomic weight of copper and ρ its density. For a current efficiency of 100%, the dimensionless thickness $\mu(x/h)/\mu_{ave}$ corresponds exactly to the value of $i(x/h)/i_{ave}$. The local current density was found to vary within a range from about $|i|$ = 1.5 to 200 mA cm^{-2} for deposition current densities of $|i_{ave}|$ = 2 to 75 mA cm^{-2}. For local current densities $|i|$

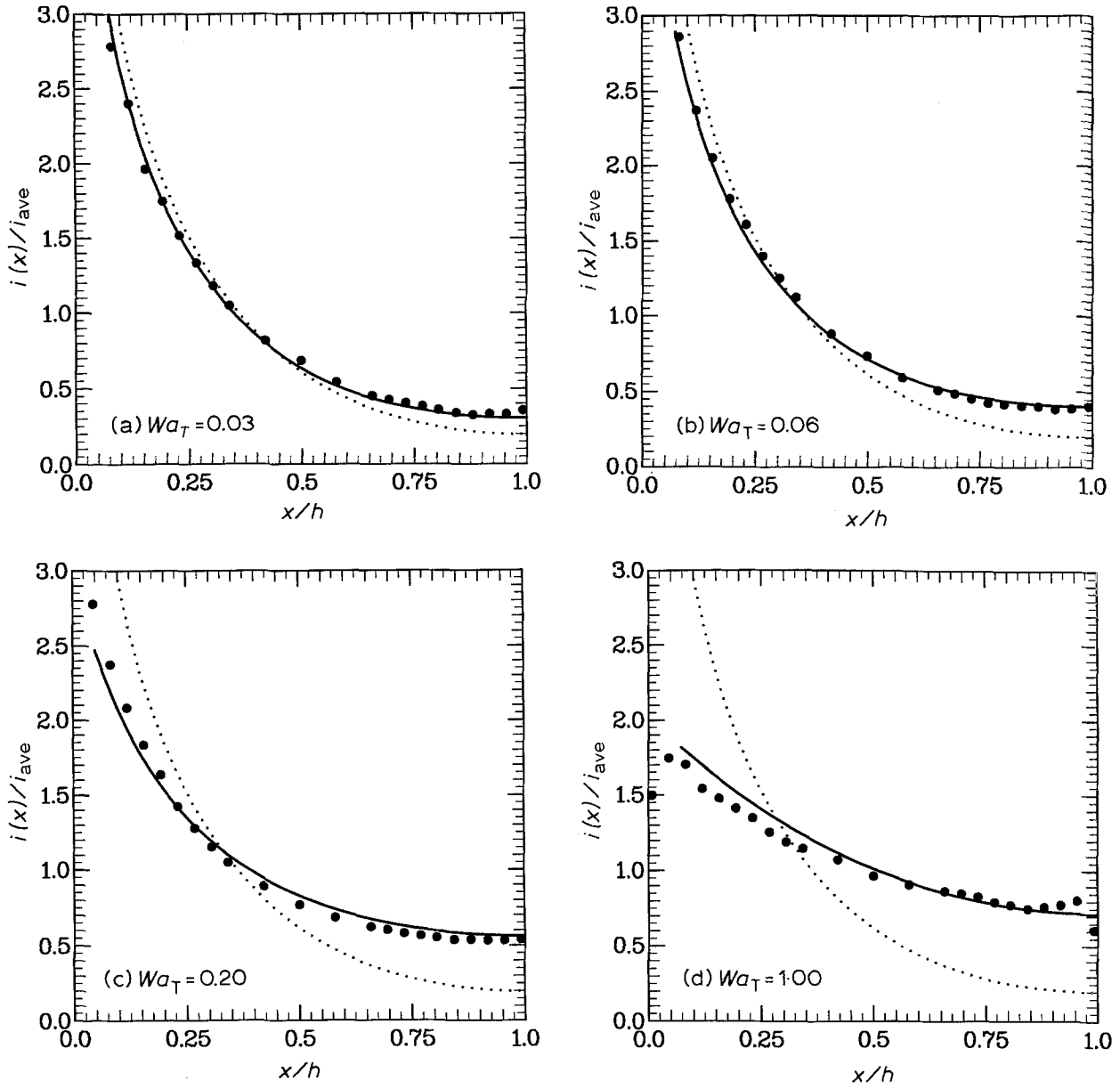

Fig. 4. The dimensionless deposit thickness μ/μ_{ave} and the dimensionless current density $i(x)/i_{ave}$ represented as a function of the dimensionless length x/h along the cathode. Wa_T: (a) 0.03; (b) 0.06; (c) 0.20 and (d) 1.00. For Wa = 0.03, the current distribution is close to the primary case. (●) Copper thickness, (——) secondary distribution, and (· · · ·) primary distribution.

up to 60 mA cm^{-2}, the deposits appear macroscopically to have a matt finish while for $|i|$ greater than 60 mA cm^{-2}, the deposits are bright.

The kinetic parameters measured experimentally were used in the secondary current distribution calculations. For Wa_T greater than 0.2 the Butler–Volmer equation was used in the calculations while for Wa_T smaller than 0.2, corresponding to higher current densities, the Tafel approximation was employed. Good agreement is found between the computed and experimental curves for Wa_T ranging from 0.03 to 0.2. A Wa_T of 0.03 yields a current distribution that is nearly primary. The theoretical primary current distribution for the RCH cell, shown in Fig. 4a, can be represented by the following analytical expression [6]:

$$\frac{i(x/h)}{i_{ave}} = \frac{0.535 - 0.458\,(x/h)}{\{0.0233 + (x/h)^2\}^{1/2}} + 8.52 \times 10^{-5} \times \exp\{7.17\,(x/h)\} \quad (12)$$

where x/h is the dimensionless distance along the cathode and $x/h = 0$ corresponds to the position of highest current density. For many practical applications of the RCH cell at low Wa_T, the above formula is sufficiently accurate for the estimation of the local current density.

5. Conclusions

A cell for electroplating studies has been built which produces a Hull cell type current distribution over a cylinder cathode rotated at controlled speed. Deposition experiments with copper confirm the theoretically calculated current distribution. The RCH cell is simple to build and, because of its uniform mass-transfer distribution, should be useful for the study of

alloy deposition and other plating processes involving a mass-transfer limited step.

Acknowledgement

Financial support for this work was provided by the Fonds National Suisse de la Recherche Scientifique and by the Office Fédéral de l'éducation et de la Science, Bern, Switzerland. The authors thank Pierre Redard from Helmut Fisher Company, Zug, Switzerland, for allowing them to use the Fischeroscope X-ray 1600/2 apparatus.

References

[1] R. O. Hull, *Am. Electroplat. Soc.* **27** (1939) 52–60.
[2] W. Hohse, 'Die Untersuchung galvanischer Bäder in der Hull Zelle', 3th ed., Eugen G. Leuze Verlag, Saulgau (1984).
[3] A. K. Graham and H. L. Pinkerton, *Proc. Am. Electroplaters Soc.* **50** (1963) 135–8.
[4] I. Kadija, J. A. Abys, V. Chinchankar and H. K. Straschil, *Plat. Surf. Finish.* **78**, July (1991) 60–7.
[5] P.-Y. Lu, *ibid.* **78**, October (1991) 62–5.
[6] C. Madore, A. C. West, M. Matlosz and D. Landolt, *Electrochim. Acta* **37** (1992) 69–74.
[7] D. R. Gabe, *J. Appl. Electrochem.* **4** (1975) 91–108.
[8] D. R. Gabe and F. C. Walsh, *ibid.* **13** (1983) 3–22.
[9] M. Eisenberg, C. W. Tobias and C. R. Wilke, *J. Electrochem. Soc.* **103** (1956) 413–16.
[10] D. J. Robinson and D. R. Gabe, *Trans. Inst. Met. Finish.* **48** (1970) 35–42.
[11] N. Ibl, *Technique de l'Ingénieur*, D902, Paris (1976).
[12] C. A. Brebbia, J. C. F. Telles et L. C. Wrobel, 'Boundary Element Techniques Theory and Applications in Engineering', Springer-Verlag, Berlin (1984).
[13] M. Matlosz, C. Creton, C. Clerc and D. Landolt, *J. Electrochem. Soc.* **134** (1987) 3015–21.
[14] M. Matlosz, O. Chène et D. Landolt, *ibid.* **137** (1990) 3033–38.
[15] O. Chène, Déposition du Cuivre en Courant Pulsé, Thèse Swiss Federal Institute of Technology, Department of Materials Science, No 820 (1989).
[16] A. C. West and J. Newman, *J. Electrochem. Soc.* **136** (1989) 2935–39.